



Asian Journal of Chemistry; Vol. 26, No. 8 (2014), 2299-2303

# ASIAN JOURNAL OF CHEMISTRY

<http://dx.doi.org/10.14233/ajchem.2014.15786>



## Design of Visible Light Response Anatase TiO<sub>2</sub>: Codoping with Transition Metals and Interstitial Carbon

SHOU-GANG CHEN, ZHEN-QING MA, MEI-YAN YU\* and WEI-WEI SUN

Institute of Materials Science and Engineering, Ocean University of China, Qingdao 266100, P.R. China

\*Corresponding author: Tel: +86 532 66781690; Email: yumeiyan@ouc.edu.cn

Received: 16 May 2013;

Accepted: 23 September 2013;

Published online: 15 April 2014;

AJC-15013

Interstitial carbon and metal codoped TiO<sub>2</sub> were theoretically studied and explaining the presence of two optical absorption thresholds in most the experiments. To bond the extra electron of interstitial carbon, we proposed the codoping system with transition metals and interstitial carbon atoms, and suggested that interstitial carbon with the nearest titanium substituted by vanadium codoped TiO<sub>2</sub> is a strong candidate for the visible light sensitive photocatalysts, with strong response absorption in both ultraviolet region and visible light region, based on the formation energy calculation and fully occupied hybridized states in the midgap.

**Keywords:** TiO<sub>2</sub>, Interstitial carbon, Dope, Photocatalyst, DFT.

### INTRODUCTION

Titanium oxide is the most popular photocatalyst due to its high photo-oxidation power, excellent stability, non-toxicity and low material cost<sup>1-3</sup>. However, the two most important shortcomings of TiO<sub>2</sub> are low efficiency of photon usage due to rapid recombination of photoexcited electron-hole pairs as well as absorption of ultraviolet irradiation only, which amounts to 5 % of solar energy<sup>4-7</sup>. In the last few years, great efforts have been made to modify the band structure of TiO<sub>2</sub> to shift its absorption edge toward the visible light region and improving its photocatalytic efficiency<sup>2</sup>. One way is to dope TiO<sub>2</sub> either with main group elements or transition metals. Monodoping with 3d transitional metal ions has been investigated extensively for enlarging the photo response of TiO<sub>2</sub> into the visible region. But it suffers from the existence of a carrier recombination center and the formation of strongly localized *d* states within the band gap, which significantly reduce carrier mobility<sup>8,9</sup>.

Doping with nonmetal atoms has been determined to be more effective than transition metal doping and nitrogen has been extensively studied both in experiments and by theories in the past few years, since Asahi *et al.*<sup>10</sup> reported the nitrogen-doped TiO<sub>2</sub>. Sakthivel and Kisch<sup>7</sup> found that the carbon-doped TiO<sub>2</sub> is more active than nitrogen-doped powder in the degradation of 4-chlorophenol by artificial light ( $\lambda = 455$  nm). They understand that the carbon impurities in TiO<sub>2</sub> maybe induce new and unexpected features, with respect to nitrogen doping. So

various experimental studies reported the carbon-doped TiO<sub>2</sub> prepared in different synthetic routes, such as flame pyrolysis of Ti metal with natural gas<sup>11,12</sup>, simple sol-gel techniques<sup>4,7,12-15</sup> and research on their absorption properties in the visible spectrum<sup>12-14,16</sup>. Correspondingly, different interpretations of the nature of the carbon doping species have been proposed. In particular, three works<sup>7,11,13</sup> have commented on the presence of two optical absorption thresholds, one in the ultraviolet (UV) region (at 3.0 eV) and one in the visible region (at 2.0 eV) and their X-ray photoelectron spectroscopy (XPS) shows that interstitial carbons (carbonate species) are the dominating states. To address the character of carbon impurities, Valentin *et al.*<sup>17</sup> used density functional theory (DFT) calculations to investigate various structural models of carbon impurities in anatase TiO<sub>2</sub> and found that under oxygen-rich conditions, interstitial carbon atoms (carbonate species) are preferred to substitutional (to oxygen) carbon and the conclusions coincide with the result of most experiments<sup>4,11-16</sup>.

Studies of carbon doped TiO<sub>2</sub> also show that the holes formed upon visible light excitation are less reactive than those formed upon UV excitation in pure TiO<sub>2</sub>, because they are trapped at midgap levels induced by carbon doping<sup>15,18,19</sup>. The visible light excited holes in the narrow band have low oxidation power in the carbon-doped systems and the hole mobility in the isolated narrow band is probably low. Therefore, the enhancements in the oxidation power and the mobility of holes are required to improve the visible light sensitivity. One method for them is to use the donor-acceptor interaction. Gai *et al.*<sup>8</sup>

proposed using passivated codoping of nonmetal and metal elements to extend the TiO<sub>2</sub> absorption edge to the visible light range. Among all the passivated codoping systems, the passivated (Mo/Cr + C)-doped TiO<sub>2</sub> with transition metal substituting on the Ti site and C substituting on the O site have much smaller band gap than other dopants. At the same time, the noncompensated anion-cation codoping is also established as an enabling concept for enhancing the visible-light photoactivity of TiO<sub>2</sub> by narrowing its band gap proposed by Zhu *et al.*<sup>20</sup> and the electrostatic attraction within the n-p dopant pair also enhances both the thermodynamic and kinetic solubility.

It is known that interstitial carbons are more preferred than substitutional carbons, especially under oxygen-rich conditions<sup>17,20</sup> according to the previous experimental and theoretical studies<sup>7,11,13,14</sup>. However, there is no detailed theoretical work involving the codoping TiO<sub>2</sub> with transition metals and interstitial carbons. For these carbonate-like doped models, transition metals are the donor to bond the extra electrons of interstitial carbons and reduce the defects of carbon doped TiO<sub>2</sub>, to the most extent. Then, it is expected that the increase in the oxidative power of holes excited by visible light and the mobility of holes, caused by the fully occupied hybridized states in the band gap which suggest that carrier recombination rates with holes may be reduced and serve to promote visible light absorption.

Based on above discussions, we designed a passivated codoping with transition metals and interstitial carbon atoms in this work and calculated the designed models using the density functional theory (DFT). Moreover, the energetic and electronic structures for these models were also studied. After analyzing the band structure and the simulated UV-visible absorption spectra of the TiO<sub>2</sub> systems, we suggested that the interstitial carbon with the nearest Ti substituted by vanadium codoped TiO<sub>2</sub> could be a strong candidate as the visible light sensitive photocatalysts, with strong response absorption in both UV and visible region.

## COMPUTATIONAL METHOD

The DFT method has proved to be very successful in modeling the ground state properties of various structures and it has been widely used to predict the structural and energetic properties. The DFT calculations in this work were carried out using the well-tested CASTEP code<sup>21</sup>, which employs ultrasoft Vanderbilt pseudopotentials<sup>22</sup> to approximate the potential field of ionic cores (including nuclei and tightly bond core electrons). The generalized gradient approximation (GGA) functions have been used with the PBE description of the correlation function<sup>23</sup>. The electron wave function was expanded in plane waves up to a cutoff energy of 380 eV and a Monkhorst-Pack k-point mesh of 3 \* 3 \* 2 was used for geometry optimization and electronic property calculations. The optimized lattice parameters for pure anatase were found to be *a* = 3.785 Å and *c* = 9.486 Å, in good agreement with experimental results (3.785 and 9.514)<sup>24</sup> indicating that our methodology is reasonable.

The doped systems were constructed from a relaxed (2 \* 2 \* 1) 48-atom anatase supercell. The interstitial carbon

doping was performed by adding one C atom in the interstitial of O octahedron (Fig. 1 a) interacting with three O atoms of anatase TiO<sub>2</sub>. Hereafter, we will refer to these interstitial carbon atoms as C<sub>i</sub>. The codoped TiO<sub>2</sub> was performed by replacing the Ti atom nearest the interstitial C with transition metal (as shown in Fig. 1b). Similarly, we will hereafter refer to these transition metals as TM<sub>Ti</sub> (such as V<sub>Ti</sub>).

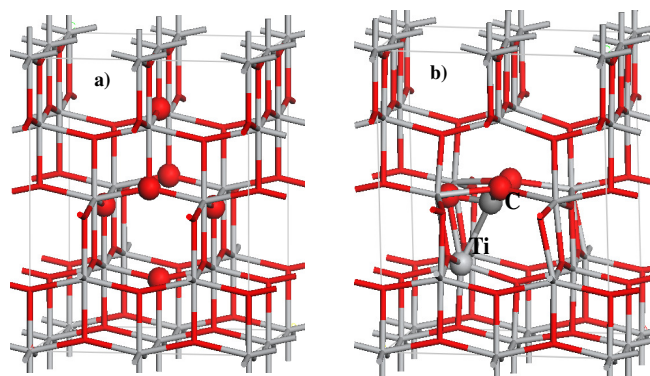


Fig. 1. Supercell model for undoped TiO<sub>2</sub> a) C<sub>i</sub> doped TiO<sub>2</sub> b) after geometry optimization. The ion doping sites are marked with N and Ta. The Ti and O atoms are presented in grey and red, respectively. And C atoms are in dark grey. Some atoms are amplified for clarity. In the (TM<sub>Ti</sub> + C<sub>i</sub>) passivated codoping, transition metals will take place of the Ti atom signed in b)

## RESULTS AND DISCUSSION

**Band-edge characters of TiO<sub>2</sub>:** To modify the band structure of TiO<sub>2</sub> by doping, we need to know the atomic wave function characters of the band-edge states. As can be seen from the total density of state (DOS) and partial density of states (PDOS) plots for bulk TiO<sub>2</sub> in Fig. 2, the valence band edge of TiO<sub>2</sub> consists mainly of O 2p states while the conduction band edge is dominated by Ti 3d states<sup>6,8</sup>. Hence, incorporation of the C and transition metal atoms should modify the valence band maximum (VBM) and conduction band minimum (CBM), respectively, due to their different p and d states with respect to O 2p and Ti 3d states.

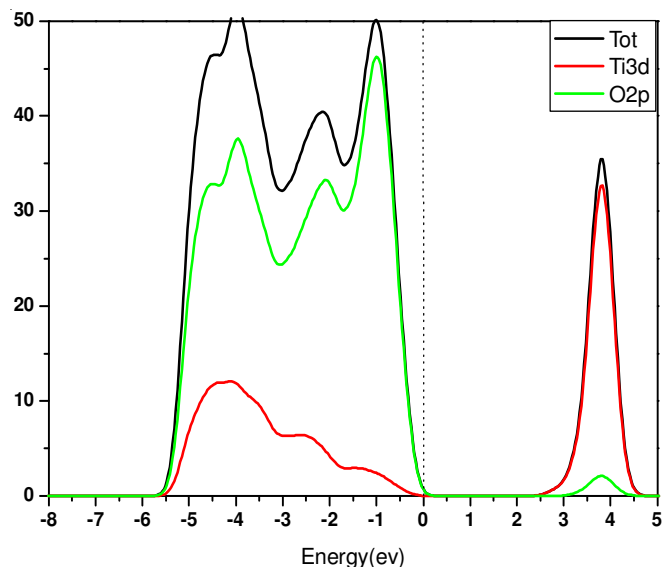


Fig. 2. The GGA -calculated DOS and partial DOS of TiO<sub>2</sub>. The highest occupied state is chosen as the Fermi energy and is set to zero

**Monodoping in TiO<sub>2</sub>:** In this study, we choose 3d transition metals vanadium and chromium and 4d transition metals niobium and molybdenum substituting on the Ti site with one or two more valence electrons than Ti as *n*-type dopants and carbon atom in the interstice of O octahedron. Fig. 3 shows the calculated DOS for monodoped TiO<sub>2</sub>. Here, the DOS in the different systems are aligned by referencing to the core levels of the atom farthest from the impurity. When transition metals (TMs) are used to substitute for Ti in TiO<sub>2</sub>, a large perturbation occurs at the CBM, which has mostly Ti *d* character. The position of the created donor state near the CBM depends on the *d* orbital energy of the dopants<sup>13</sup>. And the deep order of donor levels inside the band gap is Cr<sub>Ti</sub> > V<sub>Ti</sub> > Mo<sub>Ti</sub> > Nb<sub>Ti</sub>, with their reduction of the band gap by 0.54, 0.15, 0.03 and -0.13 eV separately, which is coincide with the results of Gai *et al.*<sup>8</sup> Because of the more delocalized character of the 4d orbital, the 4d orbital energies of Mo and Nb are close to, or higher than, that of Ti 3d. For these transition metal dopants, both V and Nb have one more valence electron than Ti, so it is single donor, whereas Cr and Mo are double donors.

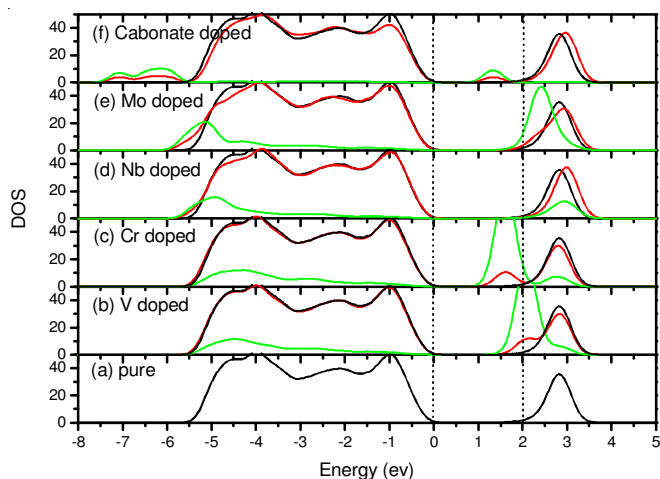


Fig. 3 The GGA -calculated total DOS for monodoped TiO<sub>2</sub> (red) compared with pure TiO<sub>2</sub> (black) and the partial DOS for impurity atoms (green). The partial DOS plots are amplified for clarity

For C<sub>i</sub> doped TiO<sub>2</sub>, the addition of one C atom in an interstitial position of 48-atoms anatase supercell (C<sub>i</sub>) results in the formation of three C-O bonds and the interaction between C<sub>i</sub> and the nearest Ti (Fig. 1b). The C-O distances are 1.415 Å for two and 1.432 Å for another and 2.202 Å for Ti-C bond which correspond to the calculated results of Valentin *et al.*<sup>17</sup>. In this configuration, carbon is formally oxidized and forms strong covalent bonds with the O atoms and this also can be indicated by the DOS (Fig. 3 f) and orbital analysis (Fig. 4 c) of C<sub>i</sub> doped TiO<sub>2</sub>, that there are three bonding C-O states below the bottom of the O 2p valence band (from -5.5 eV to -7.5 eV). The corresponding antibonding C-O states are very high in energy and fall within the TiO<sub>2</sub> conduction band. As a consequence, the excess electron introduced by the (oxidized) interstitial carbon impurity are transferred to Ti 3d states at the bottom of the conduction band (Fig. 4 b), but not to the C-O antibonding states. In this way, a new partially occupied states formed in the band gap at 0.783eV below the bottom of the conduction band (Fig. 4 a), which caused the visible light

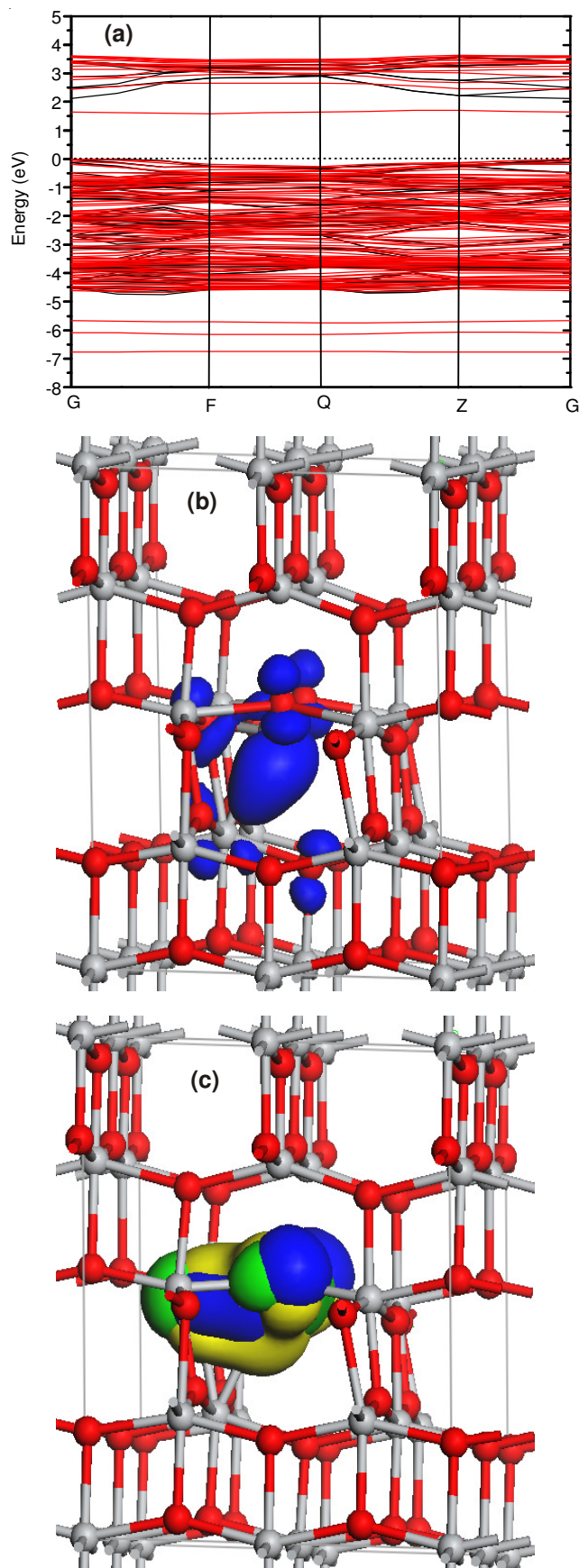


Fig. 4. Band structure (a) of undoped TiO<sub>2</sub> (black) and C<sub>i</sub> doped ones (red), and partial electron densities of (b) midgap state, and (c) the three Carbonates states below the VBM ( colored by yellow, green and blue from the top down ) of C<sub>i</sub> doped TiO<sub>2</sub>. The dashed line in (a) is the Fermi level E<sub>F</sub> of undoped TiO<sub>2</sub>



absorption (Fig. 6) by the transition of electrons from the mid gap states to the CBM. Moreover, owing to the interaction of Ti 3*d* and C<sub>1</sub>, there brings repulsion effect between the VBM and CBM of the C<sub>1</sub> doped TiO<sub>2</sub> (2.53 eV) comparing with the undoped case (2.13 eV) and this interprets the blue shift of the optical absorption threshold in the UV region respect to undoped TiO<sub>2</sub>. However, the mid gap state of C<sub>1</sub> doped TiO<sub>2</sub> is partially occupied impurity bands and it can act as trapped center of holes which are formed upon visible light excitation, so that the mobility and oxidation power of C<sub>1</sub> doped TiO<sub>2</sub> are low, this structure explain the defects of C<sub>1</sub> doped TiO<sub>2</sub> in theory and the visible light sensitivity need to be improved by passivated codoping.

**Passivated codoping in TiO<sub>2</sub>:** The above-mentioned monodoped systems create partially occupied impurity bands that can facilitate the formation of recombination centers and thus reduce the photocatalytic efficiency. Especially for interstitial C doped TiO<sub>2</sub>, the excess electron interact with Ti 3*d* forming a partial occupied impurity state. To bond the excess electron of C<sub>1</sub>, we propose to codope C<sub>1</sub> doped TiO<sub>2</sub> with different kinds of transition metals (V, Nb, Cr, Mo) with more atomic *d* orbital electrons than Ti, to act as donor levels and form electronic pairs as passivated codoping.

Fig. 5 shows the total DOS of (V<sub>Ti</sub> + C<sub>1</sub>), (Cr<sub>Ti</sub> + C<sub>1</sub>), (Nb<sub>Ti</sub> + C<sub>1</sub>) and (Mo<sub>Ti</sub> + C<sub>1</sub>)-codoped TiO<sub>2</sub> and compares the results with that for pure TiO<sub>2</sub>. We see that for (TM<sub>Ti</sub> + C<sub>1</sub>) codoped TiO<sub>2</sub> (Fig. 5 c-f), it is significant that a hybridized C<sub>1</sub> 2*p*-TM<sub>Ti</sub> 3/4*d* state is formed in the band gap, which means that fully occupied hybridized states appear in contrast to partial occupied states in single C<sub>1</sub> doping and these fully occupied hybridized states in the band gap suggest that carrier recombination rates with holes may be reduced, which would serve to promote visible light absorption.

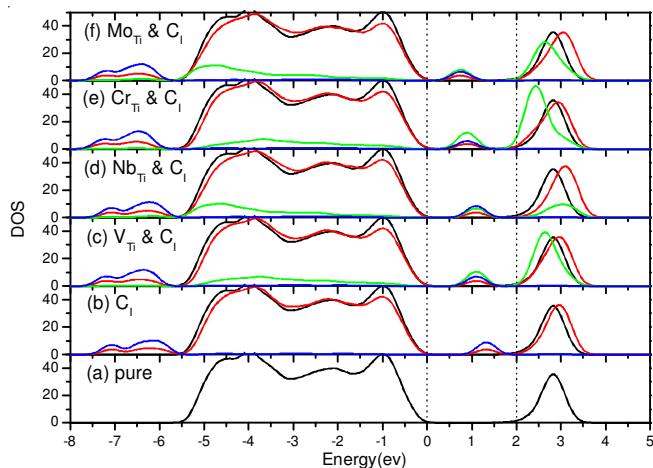


Fig. 5. The GGA- calculated total DOS for passivated codoped TiO<sub>2</sub> (red) compared with pure TiO<sub>2</sub> (black) and the partial DOS for impurity atoms (partial DOS for transition metals are in green, and C<sub>1</sub> in blue). The partial DOS plots are amplified for clarity

Moreover, owing to the repulsion effect of the TM<sub>Ti</sub> and C<sub>1</sub>, the hybridized states in the band gap move to the VBM with the increasing of the valence electrons outside the TM<sub>Ti</sub>. When displacing the Ti nearest to the C<sub>1</sub> with TM<sub>Ti</sub>, the electrons outside TM<sub>Ti</sub> interact with C<sub>1</sub> 2*p* in the form of covalent bond as well as electrovalent bond. Different from C<sub>1</sub> doped

TiO<sub>2</sub>, in which Ti-C covalent bond is the dominance, in the (TM<sub>Ti</sub> + C<sub>1</sub>) codoping TiO<sub>2</sub>, the interaction of TM<sub>Ti</sub> with C<sub>1</sub> is mainly in the form of electrovalent bond as carbonates of transition metals and to a certain extent, there is localized covalent bond. Along with the increasing of the valence electrons outside the TM<sub>Ti</sub>, the repulsion effect is rising and the gap between hybridized states and CBM is 0.738eV for C<sub>1</sub> doped TiO<sub>2</sub>, 0.960 eV for (V<sub>Ti</sub> + C<sub>1</sub>) codoped, 1.064 eV for (Nb<sub>Ti</sub> + C<sub>1</sub>) codoped, 1.111 eV for (Cr<sub>Ti</sub> + C<sub>1</sub>) codoped and 1.285 eV for (Mo<sub>Ti</sub> + C<sub>1</sub>) codoped TiO<sub>2</sub>. The gap is responsible for the visible light absorption in the UV-visible absorption spectra simulated in CASTEP calculation (Fig. 6).

On the other hand, partial TM<sub>Ti</sub> 3/4*d* states are located at the edge of the conduction band. And their effects on the bottom of CBM follow the same chemical trends as that observed in the corresponding monodoped cases. Especially for (Nb<sub>Ti</sub> + C<sub>1</sub>) codoped TiO<sub>2</sub>, the CBM obviously moves to higher energy than undoped one and this account for the weak absorption in visible light region (Fig. 6).

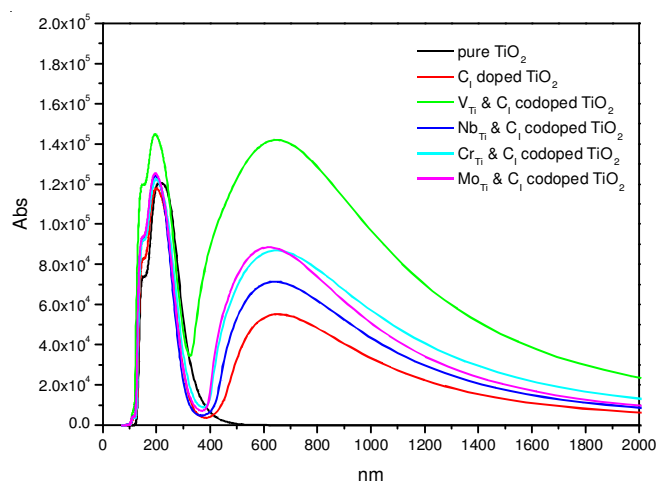


Fig. 6. The GGA-calculated UV-visible absorption spectra of undoped TiO<sub>2</sub> and passivated codoped TiO<sub>2</sub>

Fig. 6 shows the simulated UV-visible absorption spectra of the undoped and passivated codoped TiO<sub>2</sub> by the GGA-calculation. The C<sub>1</sub> doped TiO<sub>2</sub> exhibit obvious absorption in the visible region, in addition to the absorption band at wavelength below 400 nm. The former one derives from the photoelectron transition from the partially occupied states of C<sub>1</sub> in the band gap to CBM, while the later one is owing to the primary photoelectron transition from the O 2*p* (VBM) to Ti 3*d* (CBM). The optical behavior of our calculated C<sub>1</sub> doped TiO<sub>2</sub> explained the presence of two optical absorption thresholds in most experiments<sup>7,11-14</sup>.

It is also observed from the absorption spectra that (TM<sub>Ti</sub> + C<sub>1</sub>) codoped TiO<sub>2</sub> make much more absorption in the visible light region than TiO<sub>2</sub> doped with C<sub>1</sub> only. Especially the (V<sub>Ti</sub> + C<sub>1</sub>) codoped TiO<sub>2</sub> exhibits the most prominent response in both absorption regions. With one more valence electron than Ti, V can give the electron to C<sub>1</sub> and form charge-compensated donor-acceptor electrons pair to make it better photocatalytic efficiency than TiO<sub>2</sub> doped with C<sub>1</sub> only. On the other hand, (V<sub>Ti</sub> + C<sub>1</sub>) codoped TiO<sub>2</sub> has the smallest band gap which can be accounted for by the least repulsion effect in the codoped

cases. While Cr/Mo 3d/4d states are double donors with one electron bond to the excess electron of C<sub>1</sub>, while the other electron free in the system and more valence electrons will increase the repulsion effect between the hybridized states and CBM, thereby, (Cr<sub>Ti</sub> + C<sub>1</sub>) codoped and (Mo<sub>Ti</sub> + C<sub>1</sub>) codoped TiO<sub>2</sub> have relative low photocatalytic activity compared with (V<sub>Ti</sub> + C<sub>1</sub>) codoped TiO<sub>2</sub>. However, the upward moving of CBM makes (Nb<sub>Ti</sub> + C<sub>1</sub>) codoped TiO<sub>2</sub> less active than the other three ones.

### Conclusion

In summary, based on the first-principles band structure calculations and analysis of the band-edge wave function characters, we studied C<sub>1</sub> doped TiO<sub>2</sub> in theory and found the partially occupied states formed in the band gap at 0.783eV below the bottom of the conduction band, explaining the presence of two optical absorption thresholds in most experiments. To supply extra electrons to C<sub>1</sub>, we proposed passivated codoping with transition metals and interstitial carbon atoms and suggested that passivated (V<sub>Ti</sub> + C<sub>1</sub>)-doped TiO<sub>2</sub> is a strong candidate for the visible light sensitive photocatalysts, with strong response absorption in both UV region and Vis region, because there formed fully occupied hybridized states in the midgap. At the same time, the calculated formation energy (-2.75 eV) for V<sub>Ti</sub> + C<sub>1</sub> doping also favored this point at O-rich conditions according to previous paper<sup>5</sup>.

### ACKNOWLEDGEMENTS

This work was sponsored by National Natural Science Foundation (51072188).

### REFERENCES

1. L. Finegold and J. Cude, *Nature*, **238**, 38 (1972).
2. X.B. Chen and S.S. Mao, *Chem. Rev.*, **107**, 2891 (2007).
3. G.S. Wu, J.L. Wen, S. Nigro and A. Chen, *Nanotechnology*, **21**, 085701 (2010).
4. Y. Park, W. Kim, H. Park, T. Tachikawa, T. Majima and W. Choi, *Appl. Catal. B*, **91**, 355 (2009).
5. R. Long and N.J. English, *Appl. Phys. Lett.*, **94**, 132102 (2009).
6. R. Long and N.J. English, *Chem. Phys. Lett.*, **478**, 175 (2009).
7. S. Sakthivel and H. Kisch, *Angew. Chem. Int. Ed.*, **42**, 4908 (2003).
8. Y. Gai, J. Li, S. Li, J. Xia and S. Wei, *Phys. Rev. Lett.*, **102**, 036402 (2009).
9. K. Obata, H. Irie and K. Hashimoto, *Chem. Phys.*, **339**, 124 (2007).
10. R. Asahi, T. Ohwaki, K. Aoki and Y. Taga, *Science*, **293**, 269 (2001).
11. S.U.M. Khan, M. Al-Shahry and W.B. Ingler Jr., *Science*, **297**, 2243 (2002).
12. E.M. Rockafellow, X.W. Fang, B.G. Trewyn, K. Schmidt-Rohr and W.S. Jenks, *Chem. Mater.*, **21**, 1187 (2009).
13. X. Wang, S. Meng, X. Zhang, H. Wang, W. Zhong and Q. Du, *Chem. Phys. Lett.*, **444**, 292 (2007).
14. T. Ohno, T. Tsubota, K. Nishijima and Z. Miyamoto, *Chem. Lett.*, **33**, 750 (2004).
15. W.J. Ren, Z.H. Ai, F.L. Jia, L.Z. Zhang, X.X. Fan and Z.G. Zou, *Appl. Catal. B*, **69**, 138 (2007).
16. K. Obata, H. Irie and K. Hashimoto, *Chem. Phys.*, **339**, 124 (2007).
17. C. Di Valentin, G. Pacchioni and A. Selloni, *Chem. Mater.*, **17**, 6656 (2005).
18. T. Tachikawa, S. Tojo, Kawai, M. Endo, M. Fujitsuka, T. Ohno, K. Nishijima, Z. Miyamoto and T. Majima, *J. Phys. Chem. B*, **108**, 19299 (2004).
19. J. Zhong, F. Chen and J. Zhang, *J. Phys. Chem. C*, **114**, 933 (2010).
20. W. Zhu, X. Qiu, V. Iancu, X.Q. Chen, H. Pan, W. Wang, N.M. Dimitrijevic, T. Rajh, H.M. Meyer, M.P. Paranthaman, G.M. Stocks, H.H. Weitering, B. Gu, G. Eres and Z. Zhang, *Phys. Rev. Lett.*, **103**, 226401 (2009).
21. M.D. Segall, P.J.D. Lindan, M.J. Probert, C.J. Pickard, P.J. Hasnip, S.J. Clark and M.C. Payne, *J. Phys. Condens. Matter*, **14**, 2717 (2002).
22. K. Laasonen, A. Pasquarello, R. Car, C. Lee and D. Vanderbilt, *Phys. Rev. B*, **47**, 10142 (1993).
23. J.P. Perdew, K. Burke and M. Ernzerhof, *Phys. Rev. Lett.*, **77**, 3865 (1996).
24. R.W.G. Wyckoff, *Crystal Structures*, Interscience, New York, vol. 1 (1963).